https://doi.org/10.5194/egusphere-2024-1889
Preprint. Discussion started: 31 July 2024

Anthropogenic emission controls reduce summertime ozone-temperature sensitivity in the United States

Shuai Li[1,2,3], Xiao Lu[1,2,3,*], Haolin Wang[1,2,3]

[1] School of Atmospheric Sciences, Sun Yat-sen University, and Southern Marine Science and Engineering Guangdong Laboratory (Zhuhai), Zhuhai, Guangdong 519082, China

[2] Guangdong Provincial Observation and Research Station for Climate Environment and Air Quality Change in the Pearl River Estuary, Zhuhai, Guangdong 519082, China

[3] Key Laboratory of Tropical Atmosphere-Ocean System, Ministry of Education, Zhuhai, China, Zhuhai, Guangdong 519082, China

Correspondence to Xiao Lu (luxiao25@mail.sysu.edu.cn)

Abstract

The ozone-temperature sensitivity is widely used to predict the impact of future climate warming on ozone. However, trends in ozone-temperature sensitivity and possible drivers remained unclear. Here, we show that the observed summertime surface ozone-temperature sensitivity, defined as the slope of the best-fit line of daily anomaly in ozone versus maximum temperature ($m_{\Delta O3\text{-}\Delta Tmax}$), has decreased by 50% during 1990-2021 in the continental United States (CONUS), with a mean decreasing rate of -0.57 ppbv/K/decade ($p<0.01$) across 608 monitoring sites. We conduct high-resolution GEOS-Chem simulations in 1995-2017 to interpret the $m_{\Delta O3\text{-}\Delta Tmax}$ trends and underlying mechanisms in the CONUS. The simulations identify the dominant role of anthropogenic nitrogen oxides (NO_x) emission reduction in the observed $m_{\Delta O3\text{-}\Delta Tmax}$ decrease. We find that approximately 76% of the simulated decline in $m_{\Delta O3\text{-}\Delta Tmax}$ can be attributed to the temperature-indirect effects arising from the shared collinearity of other meteorological effects (such as humidity, ventilation, and transport) on ozone. The remaining portion (24%) is mostly due to the temperature-direct effects, in particular four explicit temperature-dependent processes, including the biogenic volatile organic compounds (BVOCs) emissions, soil NO_x emissions, dry deposition, and the thermal decomposition of peroxyacetyl nitrate (PAN). With reduced anthropogenic NO_x emissions, the expected ozone enhancement from temperature-driven BVOCs emissions, dry deposition, and PAN decomposition decreases, contributing to the decline in $m_{\Delta O3\text{-}\Delta Tmax.}$ However, soil NO_x emissions increase $m_{\Delta O3\text{-}\Delta Tmax}$ with anthropogenic NO_x emission reduction, indicating an increasing role of soil NO_x emissions in shaping the ozone-temperature sensitivity. As indicated by the decreased $m_{\Delta O3\text{-}\Delta Tmax}$, model simulations estimate that reduced anthropogenic NO_x emissions from 1995 to 2017 have lowered ozone enhancement from low to high temperatures by 6.8 ppbv averaged over the CONUS, significantly reducing the risk of extreme ozone pollution events under high temperatures. Our study illustrates the dependency of ozone-temperature sensitivity on anthropogenic emission levels that should be considered in the future ozone mitigation in a warmer climate.

https://doi.org/10.5194/egusphere-2024-1889
Preprint. Discussion started: 31 July 2024

1. Introduction

Surface ozone harms human health and causes loss of crop yields (Feng et al., 2022; Mills et al., 2018; Monks et al., 2015; Turner et al., 2016). It is chemically generated from its precursors including nitrogen oxides (NO_x), volatile organic compounds (VOCs), and carbon monoxide (CO) in the presence of sunlight. The natural sources, chemical kinetics, deposition, and transport of ozone and its precursors are significantly influenced by meteorology and climate (Fiore et al., 2012; Fu and Tian, 2019; Jacob and Winner, 2009; Lu et al., 2019b), shaping the strong sensitivity of surface ozone concentration to meteorological parameters such as temperature. Quantification of ozone-meteorology sensitivity provides a useful tool for predicting daily variation of ozone and for understanding climate-chemistry interactions, yet how anthropogenic emission levels may affect the sensitivity remains unclear. Here, we examine whether long-term anthropogenic control of ozone precursors has changed the response of summertime ozone to daily variations in temperature in the United States (US) and the underlying mechanisms.

High temperature is expected to increase ozone concentrations in polluted environment, through boosting biogenic VOCs (BVOCs) and soil NO_x emissions, accelerating photochemical kinetics of ozone formation, and suppressing ozone dry deposition (Hudman et al., 2012; Lin et al., 2020; Porter and Heald, 2019; Pusede et al., 2015; Romer et al., 2018; Varotsos et al., 2019). In addition, temperature-dependent meteorological parameters, such as solar radiation and humidity, and temperature-related meteorological effects, such as air stagnancy, enhanced ventilation, and regional transport, can also influence surface ozone level (Kerr et al., 2019; Lu et al., 2019b; Porter and Heald, 2019; Zhang et al., 2022a). Such effects can be reflected in but at the same time complicate the ozone-temperature relationship. Still, temperature is often used as a proxy to synthesize the effects of meteorology and climate on ozone. Previous studies have documented a robust positive ozone-temperature sensitivity in NO_x-rich environment, typically defined as the slope of the best-fit line for ozone and temperature ($d[O_3]/dT$), of 2-8 ppbv/K across the US, Europe, and China (Bloomer et al., 2009; Gu et al., 2020; Ning et al., 2022; Pusede et al., 2014; Sillman and Samson, 1995; Varotsos et al., 2019). The positive $d[O_3]/dT$ also indicates an ozone climate change penalty, *i.e.* future warming may deteriorate ozone air quality in the absence of changes in anthropogenic emission activities (Zhang et al., 2022b). The climate penalty requires additional anthropogenic emission reductions to offset the ozone increase in a warmer climate (Wu et al., 2008).

While the overall positive ozone-temperature relationship is well recognized, how ozone-temperature sensitivity has changed remains much less explored. Some studies have reported the weakening of regional ozone-temperature sensitivity in California, the Midwestern US, and the eastern US based on observations, and supposed reduction in local anthropogenic emissions as a possible driver (Bloomer et al., 2009; Jing et al., 2017; Rasmussen et al., 2013). In contrast, Fu et al. (2015) reports large interannual variations in ozone-temperature sensitivity in the southeast US that may be tied to climate variability. Model simulations project a decrease in ozone-temperature sensitivity in future scenarios with lower anthropogenic emissions in the US (Nolte et al., 2021). These studies indicate that the surface ozone-temperature sensitivity has been shifting with significant regional variations in the US, yet an up-to-date view on the long-term and continental-scale trends is currently

https://doi.org/10.5194/egusphere-2024-1889
Preprint. Discussion started: 31 July 2024

missing. In particular, the quantitative assessment of underlying mechanisms driving long-term changes in surface ozone-temperature sensitivity remains rather unclear, limiting the application of this important metric in predicting future ozone evolution.

In this study, we analyze the present-day (2017-2021) and long-term trends (1990-2021) in the summertime surface ozone-temperature sensitivity in the continental US (CONUS), combining observational monitoring network and state-of-art chemical modeling. We utilize the GEOS-Chem chemical transport model to quantify the role of anthropogenic emission reduction in the long-term trends in the ozone-temperature sensitivity, and investigate the underlying mechanisms. We also examine the benefit of reduced ozone-temperature sensitivity in ozone mitigation during high temperatures that frequently cause severe ozone pollution extremes.

2. Materials and Methods

2.1 Surface ozone measurement in the US

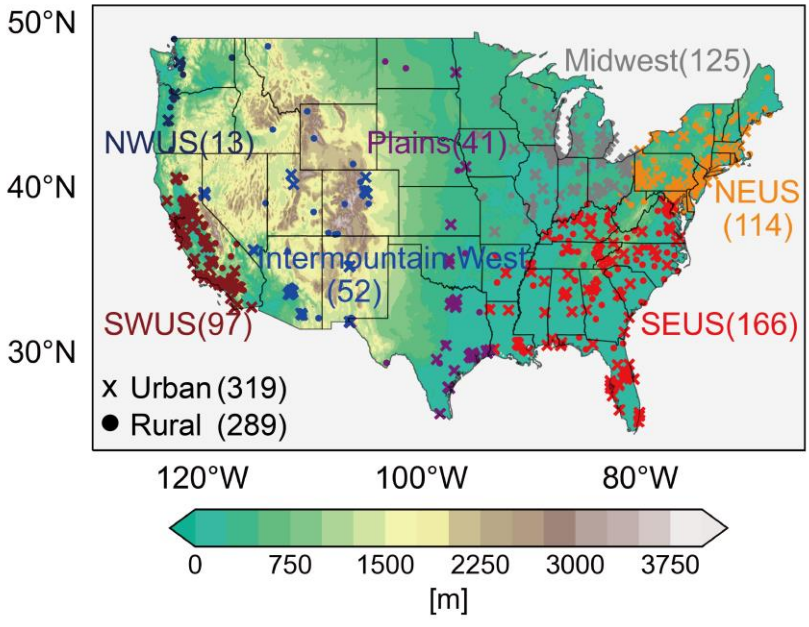

Figure 1. Locations of the 319 urban sites (crosses) and 289 rural sites (dots) across the continental US used in this study. Sites are categorized in seven regions, including Northwestern US (NWUS), Southwestern US (SWUS), Northeastern US (NEUS), Southeastern US (SEUS), Midwestern US (Midwest), the mountainous western US (Intermountain West), and Central Plains of the US (Plains). The underlying figure shows terrain elevation.

We obtain hourly measurements of surface ozone concentration from the US Environmental Pollution Agency (EPA) Air Quality System (AQS) data program. Our study period covers 1990-2021, in total of 32 years, with a focus on boreal

https://doi.org/10.5194/egusphere-2024-1889
Preprint. Discussion started: 31 July 2024

summertime (June, July, August). We derive the daily maximum 8-hour average (MDA8) ozone concentrations from the hourly data, and select sites with valid summertime ozone measurements for at least 24 years (i.e. ≥75%) in the 1990-2021 period and for at least 3 years in 2017-2021 (Text S1). A total of 608 sites are selected, including 319 urban sites and 289 rural sites (based on EPA categorization). We follow previous studies to categorize the sites into seven geographic areas (Nolte et al., 2021; Rasmussen et al., 2012), including the Northwestern US (NWUS), Southwestern US (SWUS), Northeastern US (NEUS), Southeastern US (SEUS), Midwestern US (Midwest), the mountainous western US (Intermountain West), and Central Plains of the US (Plains) (Figure 1).

2.2 Temperature data

The AQS dataset also provides measurements of temperature that could be ideally used in quantifying the ozone-temperature relationship at individual sites. However, the temperature measurement is largely missing, with only 170 sites (<30% of the total 608 sites selected for analysis) providing long-term (at least 24 years) records, which is insufficient to support our analysis. Here we derive the gridded (0.5°×0.625°) data of temperature at 2 meters above the ground from the Modern-Era Retrospective analysis for Research and Applications (Version 2, MERRA-2) dataset (Gelaro et al., 2017), which consistently serves as input for the GEOS-Chem chemical transport model (Section 2.4). We align the gridded temperature data with in-situ ozone measurement based on the coordinates of individual sites. Evaluation of the MERRA-2 gridded data with in-situ measurements of temperature at available sites shows an excellent agreement between the two with a mean bias (MB) of 0.3-1.0 K and the correlation coefficient (r) of 0.96-0.98 for years after 2000, however, the two datasets have slightly larger disparities in the earliest part of our study period (e.g. MB=0.4 K, r=0.87 for year 1990) (Figure S1).

2.3 Definition of ozone-temperature sensitivity

Our goal is to examine the response of summertime MDA8 ozone concentration to the variation in daily maximum temperature (T_{max}) across the US, and the trends in such response from 1990 to 2021. We use T_{max} instead of daytime temperature or mean temperature as strong correlation coefficients between MDA8 ozone and T_{max} have been revealed in previous studies (e.g. Steiner et al., 2010; Fu et al., 2015). Ozone levels in the US have experienced significant decreasing trends since 1980s due to anthropogenic emission control measures (Gaudel et al., 2018; Kim et al., 2006; Lin et al., 2017; Simon et al., 2015). The higher ozone concentration in earlier years may obfuscate the long-term trends in ozone-temperature sensitivity, if the ozone-temperature sensitivity were derived by the raw measurements. Therefore, we first subtract the monthly-mean MDA8 ozone concentration and T_{max} from each daily record to derive their daily anomaly (ΔO_3 and ΔT_{max}) at individual sites for each year. This process allows us to remove the seasonal (monthly) influences and also the 1990-2021 trends in ozone concentration and temperature. We then define the summertime ozone-temperature sensitivity ($m_{\Delta O3\text{-}\Delta Tmax}$) at individual sites as the slope of the best-fit line of daily ΔO_3 versus ΔT_{max}. Fu et al. (2015) also applied similar process to quantify ozone-temperature sensitivity across the southeast US. We calculate the mean values of $m_{\Delta O3\text{-}\Delta Tmax}$ over the sites

https://doi.org/10.5194/egusphere-2024-1889
Preprint. Discussion started: 31 July 2024

across the contiguous US (CONUS) or individual regions to represent the regional-mean ozone-temperature relationship. Trends in $m_{\Delta O3\text{-}\Delta Tmax}$ over each site are estimated using the linear regression method, with a 5-year smoothing average applied to the yearly $m_{\Delta O3\text{-}\Delta Tmax}$ to filter the interannual variability. The trends of the mean $m_{\Delta O3\text{-}\Delta Tmax}$ values across the sites are used to represent regional mean trends in the ozone-temperature sensitivity.

2.4 GEOS-Chem model simulation

We use the GEOC-Chem version 11-02-rc chemical transport model (Bey et al., 2001) to interpret summertime ozone-temperature sensitivity and its trend in the United States. The GEOS-Chem model is driven by MERRA-2 assimilated meteorological data. We conduct simulations over the North America nested-grid domain (140°-40° W, 10°-70° N) at the horizontal resolution of 0.5°(latitude) × 0.625°(longitude), with boundary conditions archived from consistent global simulations at 2° × 2.5° resolution. GEOS-Chem model describes a state-of-art ozone–NO_x–VOCs–aerosol–halogen tropospheric chemistry scheme, and also includes online calculation of emissions, dry and wet depositions of gases and aerosols. Anthropogenic emissions in this study are from the Community Emissions Data System (CEDS v-2021-04-21), in which the interannual variability in the US emissions are scaled based on the US National Emissions Inventory (US NEI) (McDuffie et al., 2020). The CEDS inventory indicates a significant decrease in anthropogenic NO_x, NMVOCs, CO emissions over the CONUS of 62.5, 70.8, 48.0% respectively from 1995-2017.

GEOS-Chem is capable for simulating the temperature's influences on ozone through chemical kinetics, natural emissions, transport, and dry deposition. Chemical kinetics in GEOS-Chem are modularized based on the Jet Propulsion Laboratory (JPL) and International Union of Pure and Applied Chemistry (IUPAC) scheme (IUPAC, 2011; Sander et al, 2013), with temperature input from the hourly MERRA-2 reanalysis data. GEOS-Chem also includes online calculation of temperature-dependent natural emissions. Biogenic emissions are parameterized following The Model of Emissions of Gases and Aerosols from Nature (MEGAN version v2.1) algorithm (Guenther et al., 2012), in which biogenic emissions are calculated based on temperature, solar radiation, leaf area index (LAI), and other parameters. Biogenic emissions increase exponentially with temperature, but emissions of some BVOCs are inhibited at higher temperatures. Soil NO_x emissions are calculated based on nitrogen availability in soil, edaphic conditions such as soil temperature and moisture, and other gridded parameters such as vegetation type using the Berkeley-Dalhousie Soil NO_x Parameterization as described in Hudman et al. (2012). According to the BDSNP scheme, soil emission is an exponential function of temperature when the soil temperature is between 0 and 30 °C and is constant when the soil temperature exceeds 30 °C. Some studies have shown continuous increases of soil NO_x emissions at temperature higher than 30 °C over California (Oikawa et al., 2015; Wang et al., 2021), but here we do not implement this scheme in our simulation due to the lack of supporting emissions in other regions of the CONUS. Lightning NO_x emissions are parameterized based on cloud-top heights with the spatial distribution of flash rates constrained by satellite observations (Murray et al., 2012). Biomass burning emissions are from the BB4CMIP (biomass burning emissions for CMIP6) inventory (van Marle et al., 2017), in which emissions after 1997 are consistent with the Global Fire Emissions Database version 4

https://doi.org/10.5194/egusphere-2024-1889
Preprint. Discussion started: 31 July 2024

(GFED4) inventory (van der Werf et al., 2017). However, temperature's impacts on anthropogenic NO_x and VOCs emissions (Liu et al., 2024; Wu et al., 2024) are not considered in our simulation.

Dry deposition of both gas and aerosols is calculated online based on the resistance-in-series algorithm (Wesely, 1989). Surface temperature influences deposition velocity through a stomatal resistance term, which remains low within normal temperatures (e.g. 10-30 °C) but rises at two extremes (below 0 °C and above 40 °C) (Porter and Heald, 2019), contributing to local ozone increases at high temperatures. Wet deposition for water-soluble aerosols and gas in GEOS-Chem is described by Liu et al. (2001) and Amos et al. (2012), but it has small direct effects on ozone due to the low solubility of both NO_x and ozone.

Model simulations are summarized in Table 1. We conducted a BASE simulation for July for every two years from 1995 to 2017, with one-month simulation (June) as model spin-up. The one-month spin-up time can be considered sufficient in this case as the ozone in the urban boundary layer typically has a lifetime ranging from hours to days. However, it may be short for ozone in the free troposphere where ozone has a lifetime of orders of weeks (Monks et al., 2015). The BASE simulation applies the yearly-varied anthropogenic emissions and includes all the abovementioned temperature-dependent mechanisms. We then conduct two simulations for the same 1995-2017 period, but in which the domestic anthropogenic NO_x (1995E) or VOCs (1995EAVOCs) emissions in US are fixed to 1995 level.

We conducted 14 additional sets of sensitivity experiments to explore the role of different mechanisms in the ozone-temperature sensitivity and its trend. First, we separate the effect of temperature on ozone through direct and indirect effects. Here, the temperature-direct effect is defined as the effect directly parameterized with temperature in GEOS-Chem, including natural emissions of BVOCs and soil NO_x, the chemical kinetics, dry deposition, and others. In comparison, temperature-indirect effect is defined as the effect not directly parameterized with temperature but is also influenced or reflected by temperature, for example humidity, radiation, and transport. The simulation strategy is to remove the daily variation of temperature (while keeping the diurnal cycle) and its influence on ozone daily variations. For this purpose, we generate the mean diurnal cycle of temperature averages over all 31 days in July 2017 at each grid cell. We then feed this normalized temperature data into the calculations of the GEOS-Chem (FTEMP). As such, the FTEMP simulation identifies the indirect effect of temperature on ozone. Comparison of the FTEMP simulation and BASE simulation yields a quantitative assessment of the direct effect.

For the temperature-direct effect, we further follow Porter and Heald (2019) to explore the role of four temperature-dependent mechanisms on the ozone-temperature sensitivity. These four mechanisms are BVOCs emissions, soil NO_x emissions, thermal decomposition of peroxyacetyl nitrate (PAN, whose decomposition is strongly correlated to temperature), and dry deposition. We feed the normalized temperature data (remove daily variation but keep diurnal cycle) into the calculations of all or each of the four temperature-dependent mechanisms in the GEOS-Chem. For the temperature-indirect effect, we additionally examine the role of transport in the ozone-temperature sensitivity. This is done by generating a meteorological field that retains only the daily variation of three-dimensional wind field and boundary layer height (PBLH) and removes the daily variation of all other meteorological elements, which is used into the GEOS-Chem (FTRANS).

https://doi.org/10.5194/egusphere-2024-1889
Preprint. Discussion started: 31 July 2024

We conduct the above simulations with both in 2017 and 1995 emission level, allowing us to explore the role of these mechanisms in the changes in ozone-temperature sensitivity with anthropogenic NO_x emissions reduction, which has not been addressed in previous modeling studies. Except for the BASE, 1995E, and 1995E-AVOCs simulation, other simulations are only conducted for year 2017 (the latest year with available anthropogenic emission inventory when the simulations were conducted) as sensitivity tests.

Table 1 Configurations of Model Simulations

Cases	Simulation time	Description
BASE	July,1995-2017 (biennially)	Default simulation with yearly-varied anthropogenic emissions and all temperature-dependent mechanisms
1995E	Same as BASE	Same as BASE, but anthropogenic NO_x emissions fixed in 1995
1995EAVOCs	Same as BASE	Same as BASE, but anthropogenic VOCs emissions fixed in 1995
BASE-FTEMP	July, 2017	Same as BASE, but with normalized temperature field in the model
1995E-FTEMP	July, 2017	Same as 1995E, but with normalized temperature field in the model
BASE-FTRANS	July, 2017	Same as BASE, but with normalized all meteorological elements except three-dimensional wind field and PBLH
1995E-FTRANS	July, 2017	Same as 1995E, but with normalized all meteorological elements except three-dimensional wind field and PBLH
BASE-FALL	July, 2017	Same as BASE, but remove four mechanisms temperature dependence by normalized temperature for BVOCs emissions, Soil NO_x emissions, PAN decomposition, and dry deposition
1995E-FALL	July, 2017	Same as 1995E, but remove four mechanisms temperature dependence by normalized temperature for BVOCs emissions, Soil NO_x emissions, PAN decomposition, and dry deposition
BASE-FBVOC	July, 2017	Same as BASE, but remove BVOCs temperature dependence by normalized temperature for biogenic VOC emissions
1995E -FBVOC	July, 2017	Same as 1995E, but remove BVOCs temperature dependence by normalized temperature for biogenic VOC emissions
BASE-FSNO$_x$	July, 2017	Same as BASE, but remove Soil NO_x temperature dependence by normalized temperature for soil NO_x emissions

https://doi.org/10.5194/egusphere-2024-1889
Preprint. Discussion started: 31 July 2024

1995E-FSNO$_x$	July, 2017	Same as 1995E, but remove Soil NO$_x$ temperature dependence by normalized temperature for soil NO$_x$ emissions
BASE-FPAN	July, 2017	Same as BASE, but remove PAN temperature dependence by normalized temperature for PAN decomposition
1995E-FPAN	July, 2017	Same as 1995E, but remove PAN temperature dependence by normalized temperature for PAN decomposition
BASE-FDEP	July, 2017	Same as BASE, but remove dry deposition temperature dependence by normalized temperature for dry deposition
1995E-FDEP	July, 2017	Same as 1995E, but remove dry deposition temperature dependence by normalized temperature for dry deposition

3. Results

3.1 Present-day level and trends of summertime ozone-temperature sensitivity in the continental US

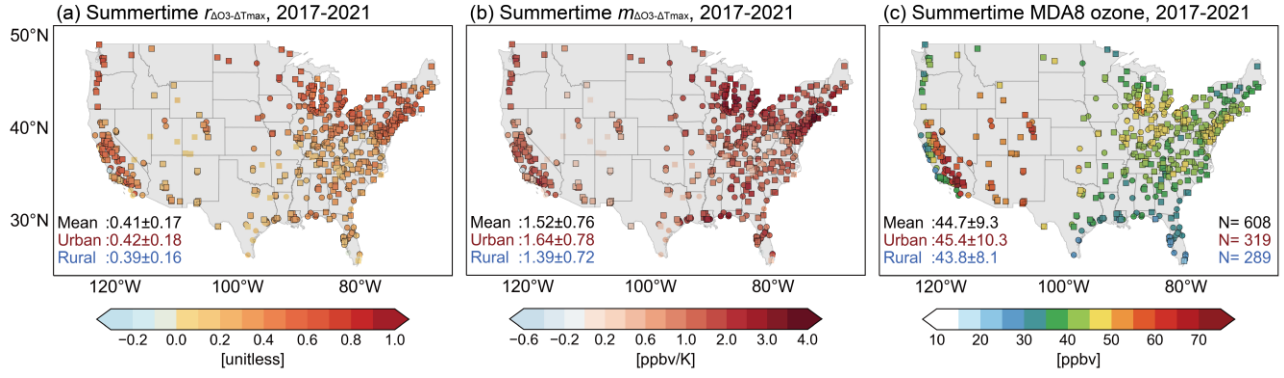

Figure 2. Present-day summertime ozone concentrations and ozone-temperature sensitivity in the continental US. (a,b) Distribution of summertime (June, July, August) $r_{\Delta O3\text{-}\Delta Tmax}$ and $m_{\Delta O3\text{-}\Delta Tmax}$ at individual sites averaged in 2017-2021. Black boarders indicate sites with a p-value<0.01 for $r_{\Delta O3\text{-}\Delta Tmax}$ or $m_{\Delta O3\text{-}\Delta Tmax}$. (c) Summer mean MDA8 ozone concentrations at individual sites. Urban sites are represented by circle and rural sites by square. Mean values and standard deviations over the sites are shown in the inset.

Figure 2(a) presents the widespread positive correlation coefficients between summertime daily MDA8 ozone and T_{max} ($r_{\Delta O3\text{-}\Delta tmax}$) across the CONUS sites. 604 out of the total 608 sites are showing positive $r_{\Delta O3\text{-}\Delta Tmax}$ (570 sites with p-value<0.01) in the present-day (2017-2021), with a mean $r_{\Delta O3\text{-}\Delta Tmax}$ value of 0.41±0.17 (mean ± standard deviation across the sites) averaged over all sites. Urban sites show slightly higher $r_{\Delta O3\text{-}\Delta Tmax}$ values than rural sites. Figure 2(b) shows that the present-day mean

https://doi.org/10.5194/egusphere-2024-1889
Preprint. Discussion started: 31 July 2024

$m_{\Delta O3\text{-}\Delta Tmax}$ (see Section 2.3 for the definition) values averaged for the 608 sites are 1.52±0.76 ppbv/K, with the $m_{\Delta O3\text{-}\Delta Tmax}$ values at urban sites higher by 18% than those averaged for the rural sites (1.64±0.78 versus 1.39±0.72 ppbv/K). These results reflect the expected ozone increases with temperature in NO_x-rich environment, which are more commonly found in urban than rural areas.

We find distinct variability in the spatial distributions of both $r_{\Delta O3\text{-}\Delta Tmax}$ and $m_{\Delta O3\text{-}\Delta Tmax}$ (Figure 2, Table S1). The Midwest and NEUS regions show the highest mean $m_{\Delta O3\text{-}\Delta Tmax}$ values reaching 2.07±0.61 ($r_{\Delta O3\text{-}\Delta Tmax}$=0.50±0.12) and 1.96±0.65 ppbv/K ($r_{\Delta O3\text{-}\Delta Tmax}$=0.52±0.09), followed by NWUS with mean $m_{\Delta O3\text{-}\Delta Tmax}$ of 1.54±0.39 ppbv/K ($r_{\Delta O3\text{-}\Delta Tmax}$=0.63±0.08). The Intermountain West and Plains region show the lowest mean $m_{\Delta O3\text{-}\Delta Tmax}$ of less than 1.1 ppbv/K in both urban and rural sites with mean $r_{\Delta O3\text{-}\Delta Tmax}$ lower than 0.25, indicating daily ozone variation in this region is not strongly affected by temperature. We also find that the spatial distribution of ozone-temperature sensitivity does not follow that of the MDA8 ozone level (Figure 2c), as the highest summertime MDA8 ozone concentrations are over the SWUS and Intermountain West Regions. The higher $m_{\Delta O3\text{-}\Delta Tmax}$ in the NEUS and Midwest regions than in other regions may reflect the stronger daily variation of ozone due to rapid shift of synoptic patterns (e.g. mid-latitude cyclones) in this region during summer (Leibensperger et al., 2008). The low $m_{\Delta O3\text{-}\Delta Tmax}$ in the Intermountain region largely reflects the strong background ozone influences (including stratospheric intrusion, long-range transport of wildfire or anthropogenic plumes) instead of local photochemical production (Jaffe et al., 2018; Zhang et al., 2014). These background sources may contribute to high ozone there but are not directly modulated by local temperature.

Previous studies report a decrease in ozone concentration at extreme high temperature over the US (Shen et al., 2016; Steiner et al., 2010). Here we investigate how the suppression of ozone concentration influences the overall ozone-temperature sensitivity. We identify occurrences of ozone suppression and the critical temperature (i.e. beyond which ozone increases are suppressed) at individual sites every year following the criteria described in Ning et al (2022). We find that while ozone suppression at extreme high temperature can be detected at 477 out of 608 sites in 2017-2021, excluding data above the critical temperature only changes the present-day mean $m_{\Delta O3\text{-}\Delta Tmax}$ by 2.6%. It indicates that such phenomenon does not change the overall positive ozone-temperature sensitivity.

https://doi.org/10.5194/egusphere-2024-1889
Preprint. Discussion started: 31 July 2024

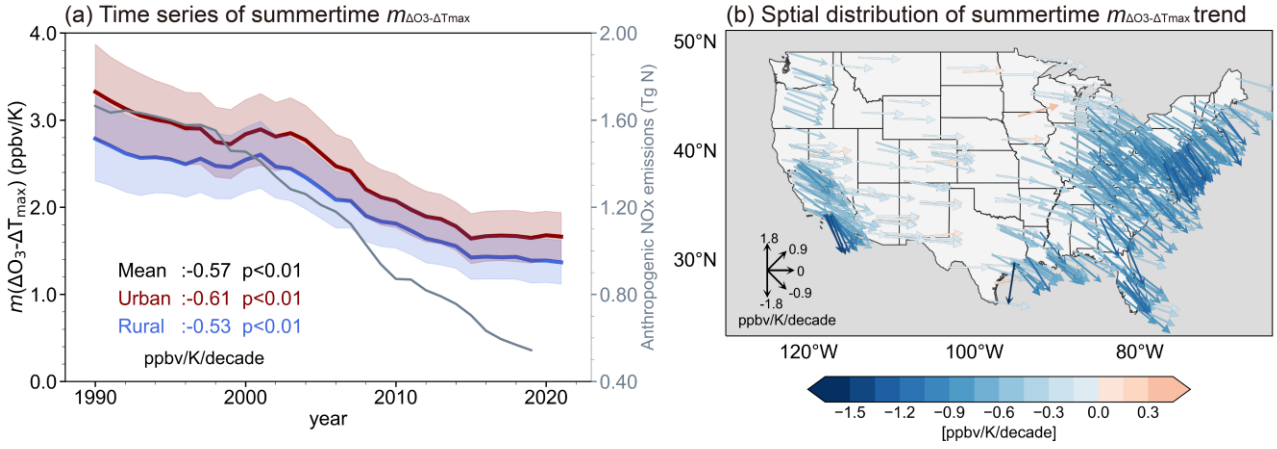

Figure 3. Observed decrease in summertime ozone-temperature sensitivity in 1990-2021. (a) Time series of the summertime $m_{\Delta O3\text{-}\Delta Tmax}$ averaged over the CONUS sites, with a 5-year smoothing average applied to the yearly $m_{\Delta O3\text{-}\Delta Tmax}$ to filter the interannual variability. $m_{\Delta O3\text{-}\Delta Tmax}$ for urban and rural sites are shown in red and blue lines, respectively. Shaded areas represent the range of mean values ± 30% of standard deviation across the sites. The CONUS $m_{\Delta O3\text{-}\Delta Tmax}$ trends are shown inset. Anthropogenic NO_x emissions in the CONUS are shown in grey line. (b) Spatial distributions of long-term trends in $m_{\Delta O3\text{-}\Delta Tmax}$ in 1990-2021 across the US. Both directions and colors of the vectors indicate the $m_{\Delta O3\text{-}\Delta Tmax}$ trends.

The present-day (2017-2021) ozone-temperature sensitivity is lower than the reported values for earlier years (i.e. 2-7 ppbv/K reported in 2000 (Bloomer et al., 2009; Fu et al., 2015; Rasmussen et al., 2013), though different definitions of ozone-sensitivity sensitivity were applied), suggesting that the ozone-temperature sensitivity may have experienced significant reduction in recent decades. Figure 3 illustrates this feature from long-term observations in 1990-2021. We find in Figure 3a that mean $m_{\Delta O3\text{-}\Delta Tmax}$ for the CONUS decreased by 50% from 3.0 ppbv/K in 1990 to 1.5 ppbv/K in 2021 with a mean decreasing rate of -0.57 ppbv/K/decade ($p<0.01$). $m_{\Delta O3\text{-}\Delta Tmax}$ over the CONUS urban sites was higher than rural sites by 0.50 ppbv/K in the early 1990s. However, urban sites exhibit a faster decline rate of $m_{\Delta O3\text{-}\Delta Tmax}$ (-0.61 ppbv/K/decade, $p<0.01$) compared to rural (-0.53 ppbv/K/decade, $p<0.01$), narrowing the disparity in $m_{\Delta O3\text{-}\Delta Tmax}$ between the two. At the same time, the mean $r_{\Delta O3\text{-}\Delta Tmax}$ decreased from 0.51 in 1990 to 0.40 in 2021 (Figure S2). The significant decrease in both $m_{\Delta O3\text{-}\Delta Tmax}$ and $r_{\Delta O3\text{-}\Delta Tmax}$ all imply a much weaker response of ozone to temperature in present-day compared to that in three decades ago. While some studies have shown observed decreases in some regions (e.g. California as described in Steiner et al. (2010)), such significant decreases of ozone-temperature sensitivity over the CONUS have not been presented in previous studies to the best of our knowledge.

The decreasing trends in $m_{\Delta O3\text{-}\Delta Tmax}$ are widespread across the CONUS sites (Figure 3b), but spatial and temporal variabilities exist. 411 sites (68%) out of the total 608 sites are showing negative trends with $p<0.01$(481 sites with $p<0.05$). The largest decreases are in the NEUS region, where $m_{\Delta O3\text{-}\Delta Tmax}$ values exceeded 4.3 ppbv/K in the 1990s but have steadily decreased by -0.83 ppbv/K/decade, reaching 1.7 ppbv/K in 2021. The SWUS region also shows a large decrease in $m_{\Delta O3\text{-}\Delta Tmax}$ by -0.60 ppbv/K/decade($p<0.01$). A distinct feature in the SWUS is the notably high urban-rural disparity in $m_{\Delta O3\text{-}\Delta Tmax}$ (4.7 versus 1.9 ppbv/K) in the early 1990s (Figure S3), but this disparity has been significantly reduced as urban sites exhibit a

https://doi.org/10.5194/egusphere-2024-1889
Preprint. Discussion started: 31 July 2024

much larger $m_{\Delta O3\text{-}\Delta Tmax}$ trend (-0.88 ppbv/K/decade, p<0.01) than rural sites (-0.34 ppbv/K/decade, p<0.01), particularly in early 1990s. The SEUS and Midwest regions also show decreases in $m_{\Delta O3\text{-}\Delta Tmax}$ with a mean rate of -0.61 and -0.52 ppbv/K. However, we notice an increase of $m_{\Delta O3\text{-}\Delta Tmax}$ in 1990-2000 for the SEUS region and in 1990-2005 for the Plains region (Figure S3). Fu et al. (2015) attributes the increase ozone-temperature sensitivity in 1990-2000 in the SEUS to variations in regional ozone advection tied to climate variability. The region with the least $m_{\Delta O3\text{-}\Delta Tmax}$ trends is the Intermountain region (-0.08 ppbv/K/decade).

3.2 Simulated long-term trends in ozone-temperature sensitivity and attribution to anthropogenic emission reduction

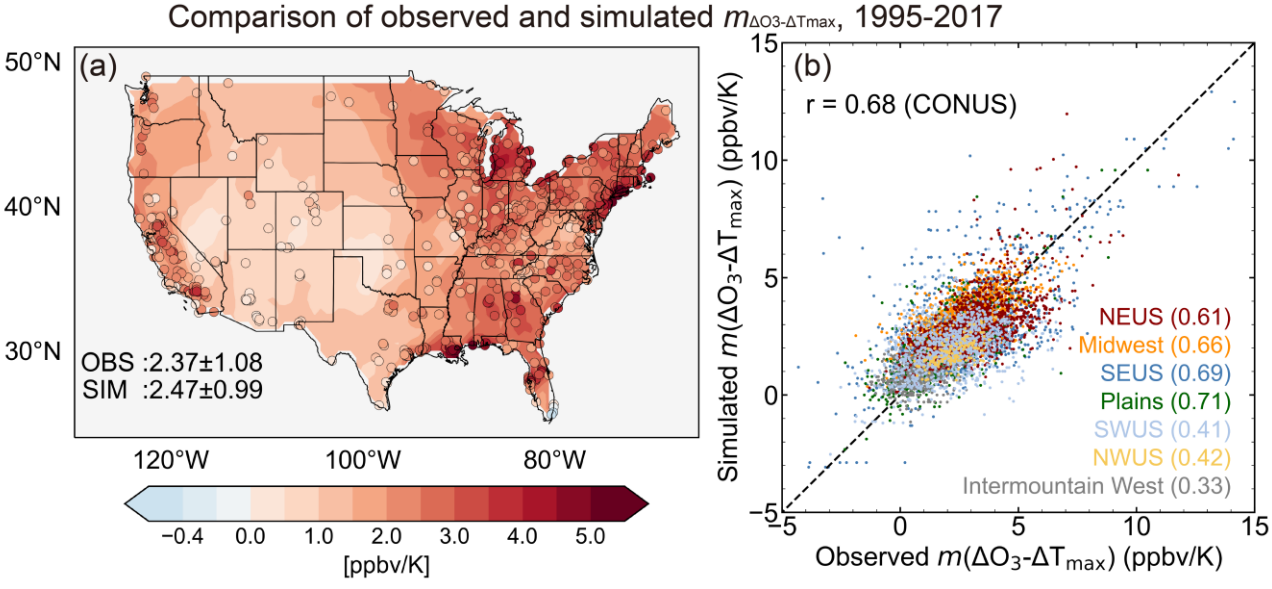

Figure 4. Evaluation of GEOS-Chem simulated $m_{\Delta O3\text{-}\Delta Tmax}$ in July, 1995-2017. (a) Spatial distributions of the observed (circles) and simulated (from the BASE simulation, shaded) $m_{\Delta O3\text{-}\Delta Tmax}$ during July averaged over 1995 to 2017. (b) Scatterplots of the observed and simulated $m_{\Delta O3\text{-}\Delta Tmax}$ for July in each simulated year from 1995 to 2017. Mean values, standard deviations for the CONUS sites from the observation and GEOS-Chem model, and their correlation coefficients (r) in different regions are shown in the inset.

We now apply the GEOS-Chem chemical transport model to interpret the trends in ozone-temperature sensitivity over the CONUS. Figure S5 compares the spatial distribution of observed and simulated mean surface MDA8 ozone concentrations in July at the 608 sites averaged for 12 years (1995-2017 biennially). Our GEOS-Chem simulation captures the spatial distributions of surface MDA8 ozone across the CONUS, although showing some high bias of MDA8 ozone of 11 ppbv, as also reported in other surface ozone air quality studies using the GEOS-Chem model (Lu et al., 2019a; Travis and Jacob, 2019). Most importantly, the model largely reproduces the spatial pattern of observed $m_{\Delta O3\text{-}\Delta Tmax}$, with a high correlation coefficient of 0.68 and a small positive mean bias of 0.10 ppbv/K (4%) at the 608 sites for the monthly $m_{\Delta O3\text{-}\Delta Tmax}$ values at all sites (Figure

https://doi.org/10.5194/egusphere-2024-1889
Preprint. Discussion started: 31 July 2024

4). Table S2 further shows the simulated and observed $m_{\Delta O3\text{-}\Delta Tmax}$ and their correlation coefficients (r) across different periods and regions. The model demonstrates relatively better performance of $m_{\Delta O3\text{-}\Delta Tmax}$ across the CONUS in 2001-2011 compared to other periods, with small mean absolute bias (0.03-0.18 ppbv/K, 1%-8%) and high correlation coefficients (0.67-0.71). The simulated $m_{\Delta O3\text{-}\Delta Tmax}$ in the Eastern United States (NEUS, SEUS, Midwest, and Plains) is in better agreement with the observed values than in the Western United States, with *r* ranging from 0.49 to 0.79. The above analyses support that the GEOS-Chem model well captures the overall ozone-temperature sensitivity in the period of 1995-2017.

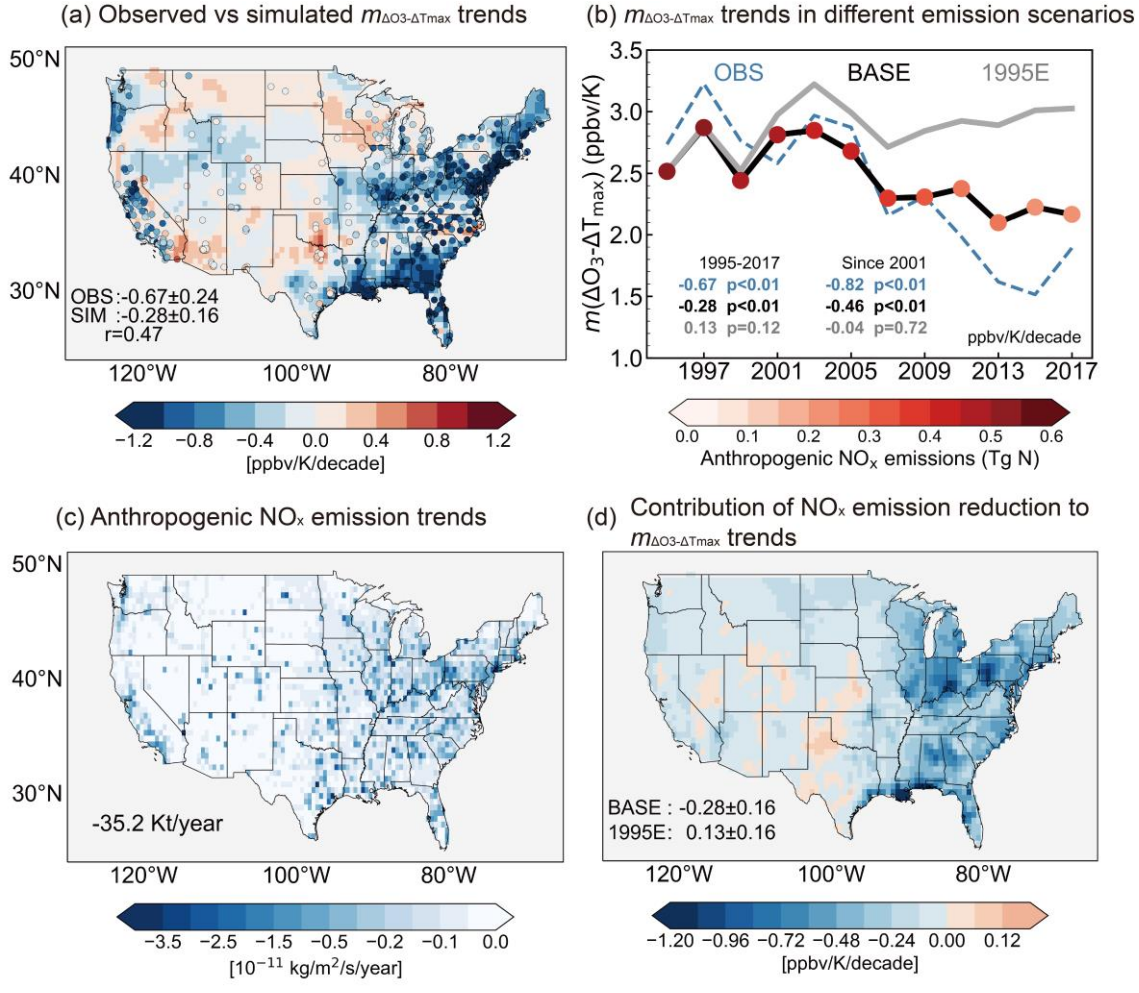

Figure 5. GEOS-Chem simulated decrease in summertime ozone-temperature sensitivity and the attribution to reduction in anthropogenic NO_x emission. (a) Spatial distributions of the observed (circles) and simulated (from the BASE simulation, shaded) $m_{\Delta O3\text{-}\Delta Tmax}$ trends during July from 1995 to 2017. Mean trends±95% confidence level for the CONUS sites from the observation and GEOS-Chem model, and the correlation coefficients (*r*) of $m_{\Delta O3\text{-}\Delta Tmax}$ trends between the two are shown inset. (b) Time series of the observed and simulated $m_{\Delta O3\text{-}\Delta Tmax}$ in July during 1995-2017 (biennially) at CONUS sites. Results from the BASE simulation and a sensitivity simulation with anthropogenic NO_x emissions fixed at 1995 level (1995E) are compared. Colored circles denote the July

https://doi.org/10.5194/egusphere-2024-1889
Preprint. Discussion started: 31 July 2024

anthropogenic NO_x emissions in the CONUS. (c) Spatial distribution of anthropogenic NO_x emission trends during July from 1995 to 2017. Trends are calculated for each model grid. Emissions trends aggregated over the CONUS are insets. (d) Contribution of anthropogenic NO_x emissions to $m_{\Delta O3\text{-}\Delta Tmax}$ trends, estimated as the difference in the $m_{\Delta O3\text{-}\Delta Tmax}$ trend between BASE and 1995E simulations. Mean trends±95% confidence level is shown inset.

Figure 5(a) further compares the observed and GEOS-Chem simulated 1995-2017 trends in $m_{\Delta O3\text{-}\Delta Tmax}$ in July across the CONUS. The following analysis applies biennial data from 1995 to 2017 to align with the GEOS-Chem simulations. The overall observed $m_{\Delta O3\text{-}\Delta Tmax}$ trends in July, as depicted in Figure 5a, are similar to those in June-July-August period as presented in Figure 3b, but there are slight differences at individual sites reflecting the difference in the time frame. We find that driven by yearly-varied meteorological fields and anthropogenic emissions, GEOS-Chem model successfully reproduces the decline of $m_{\Delta O3\text{-}\Delta Tmax}$ across the CONUS, showing a spatial correlation coefficient of 0.47 with observed $m_{\Delta O3\text{-}\Delta Tmax}$ trends ($p<0.01$). In particular, the model reproduces the much larger $m_{\Delta O3\text{-}\Delta Tmax}$ decreases in the eastern CONUS (the NEUS, Midwest, and SEUS) compared to other regions, consistent with the observations. However, the model has difficulty in capturing the magnitude of observed $m_{\Delta O3\text{-}\Delta Tmax}$ trends. The model shows a mean $m_{\Delta O3\text{-}\Delta Tmax}$ trend of -0.28 ppbv/K/decade over the CONUS that accounts for 42% of the observed trends of -0.67 ppbv/K/decade. This largely reflects the model's bias in capturing the $m_{\Delta O3\text{-}\Delta Tmax}$ decreases in the SWUS region. Figure 5b also shows that the model's underestimation of $m_{\Delta O3\text{-}\Delta Tmax}$ trends is primarily attributed to an overestimation of $m_{\Delta O3\text{-}\Delta Tmax}$ from 2013 to 2017 and an underestimation from 1995 to 1999. The underestimation of $m_{\Delta O3\text{-}\Delta Tmax}$ from 1995 to 1999 may be partly attributed to the bias in MERRA-2 temperature dataset such that the observed $m_{\Delta O3\text{-}\Delta Tmax}$ may be biased (Figure S1). Excluding the 1995, 1997, and 1999 records improve the model's ability in capturing observed $m_{\Delta O3\text{-}\Delta Tmax}$ trends (-0.46 ppbv/K/decade in GEOS-Chem vs -0.82 ppbv/K/decade, 56%), especially for the SWUS region (Figure 5b, Figure S7). We do not further differentiate the simulated $m_{\Delta O3\text{-}\Delta Tmax}$ trends at urban and rural sites because the model resolution at about 50 km may be too coarse for such separation.

Previous studies have implied reductions of anthropogenic emissions would result in a decrease in the ozone-temperature sensitivity (Bloomer et al., 2009). Here we explicitly test this propose by our sensitivity experiments with anthropogenic NO_x emissions in US fixed at the 1995 level (1995E). Figure 5b shows that once the anthropogenic NO_x emissions were fixed in 1995, the GEOS-Chem would simulate no decrease in $m_{\Delta O3\text{-}\Delta Tmax}$ (instead a positive trend by 0.13 ppbv/K/decade averaged over all sites, $p=0.12$). This implies that the change in anthropogenic NO_x emissions alone decreases $m_{\Delta O3\text{-}\Delta Tmax}$ by -0.41 ppbv/K/decade for all 608 sites, compared to the observed $m_{\Delta O3\text{-}\Delta Tmax}$ trend of -0.67 ppbv/K/decade, and is apparently the dominant driver of the observed decrease in $m_{\Delta O3\text{-}\Delta Tmax}$. In comparison, the simulation with only anthropogenic VOCs emissions fixed at the 1995 level shows neglectable difference in $m_{\Delta O3\text{-}\Delta Tmax}$ compared to the BASE simulation. We note that the difference in $m_{\Delta O3\text{-}\Delta Tmax}$ trend between BASE and 1995E simulations is highly consistent with the spatial distribution of anthropogenic NO_x emission trends ($r=0.40$, $p<0.01$) (Figure 5c), further confirming that NO_x emission reduction is an important driver of the decline in $m_{\Delta O3\text{-}\Delta Tmax}$. Figure S7 illustrates that the regions with $m_{\Delta O3\text{-}\Delta Tmax}$ being mostly affected by anthropogenic NO_x emission reductions are located in the eastern CONUS (the NEUS, Midwest, and SEUS), while other regions are less affected.

https://doi.org/10.5194/egusphere-2024-1889
Preprint. Discussion started: 31 July 2024

3.3 The underlying mechanisms for the decrease in ozone-temperature sensitivity with reduced NO_x emissions

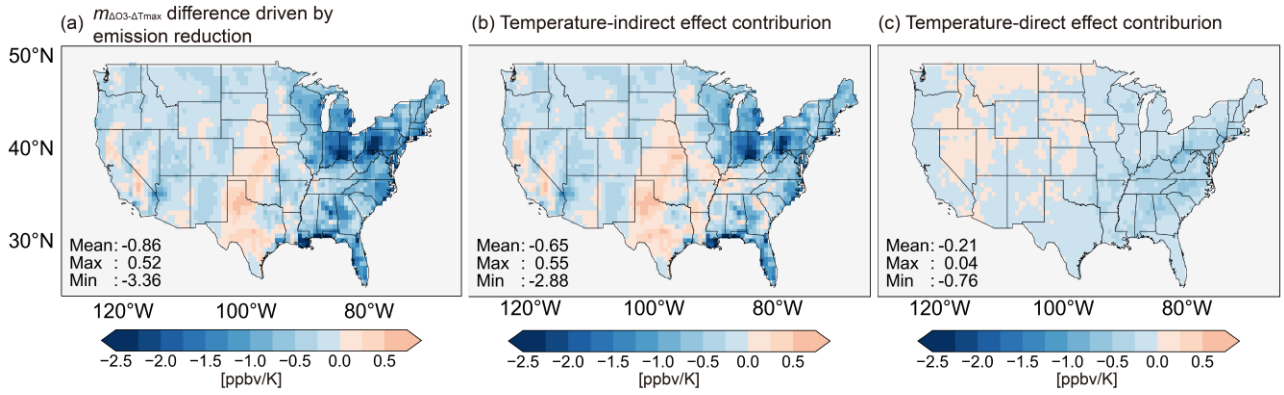

Figure 6. Mechanisms for the decrease in $m_{\Delta O3\text{-}\Delta Tmax}$ with anthropogenic NO_x emission reduction. (a) Changes in $m_{\Delta O3\text{-}\Delta Tmax}$ due to the difference in anthropogenic NO_x emissions in 2017 and 1995, estimated as the difference in $m_{\Delta O3\text{-}\Delta Tmax}$ between the BASE and 1995E simulation for July 2017. (b) The contribution of the temperature-indirect effect to $m_{\Delta O3\text{-}\Delta Tmax}$ with changes in anthropogenic NO_x emissions, estimated as the difference of $m_{\Delta O3\text{-}\Delta Tmax}$ between BASE-FTEMP and 1995E-FTEMP (Section 2.4). (c) The contribution of the temperature-direct effect, estimated as the difference of $m_{\Delta O3\text{-}\Delta Tmax}$ between BASE and 1995E minus the difference between BASE-FTEMP and 1995E-FTEMP. Mean, maximum, and minimum values of the contributions among all CONUS sites are shown inset.

Our analyses above prove that the reduction in anthropogenic NO_x emissions is the dominant driver of the observed long-term decrease in $m_{\Delta O3\text{-}\Delta Tmax}$ in the CONUS. We next examine how the changes in anthropogenic NO_x emissions have altered processes controlling ozone's response to temperature. Previous studies have shown that temperature's impacts on surface ozone concentrations involve acceleration of chemical reaction rates, in particular the thermal decomposition of PAN, increased natural emissions of BVOCs and soil reactive nitrogen, and inhabitation of ozone dry deposition (Lu et al., 2019b; Porter and Heald, 2019; Steiner et al., 2010). Some studies also argued that the temperature-related covariance with other meteorological phenomena such as drought (low humidity), stagnancy, and transport may be more important in determining $m_{\Delta O3\text{-}\Delta Tmax}$ (Kerr et al., 2019; Porter and Heald, 2019; Zhang et al., 2022a, c). Based on these previous studies, we focus on the changes of these impacts on $m_{\Delta O3\text{-}\Delta Tmax}$ with anthropogenic emission reduction in the US.

We illustrate in Figure 6 the simulated changes in $m_{\Delta O3\text{-}\Delta Tmax}$ in July 2017 through temperature-direct effects and temperature-indirect effects associated with the anthropogenic reduction of NO_x. Figure 6a shows that the reduction of anthropogenic NO_x emissions from 1995 to 2017 alone decreased $m_{\Delta O3\text{-}\Delta Tmax}$ by 0.86 ppbv/K in July 2017 (estimated as the difference between the BASE simulation and 1995E simulation). The decreases are larger in the eastern US (including NEUS, Midwest, and SEUS), reaching 1.37, 1.28, and 1.00 ppbv/K, respectively. When the temperature-direct effect is all removed

https://doi.org/10.5194/egusphere-2024-1889
Preprint. Discussion started: 31 July 2024

from the GEOS-Chem simulation (Section 2.4), the reduction of anthropogenic NO_x emissions from 1995 to 2017 would decrease $m_{\Delta O3\text{-}\Delta Tmax}$ by 0.65 ppbv/K in July 2017. It indicates that only a relatively small portion of the decrease in $m_{\Delta O3\text{-}\Delta Tmax}$ (24%, 0.21 ppbv/K compared with 0.86 ppbv/K) with anthropogenic NO_x reduction can be attributed to the temperature-direct effect (Figure 6c), yet the remaining is explained by temperature-indirect effect. Our results agree with Porter and Heald (2019), which shows that the collinearity between temperature and other meteorological variables played a significant role in determining the overall ozone-temperature relationship. Here, we further demonstrate that the temperature-indirect effect also dominates the decline in ozone-temperature sensitivity with anthropogenic NO_x emission reduction.

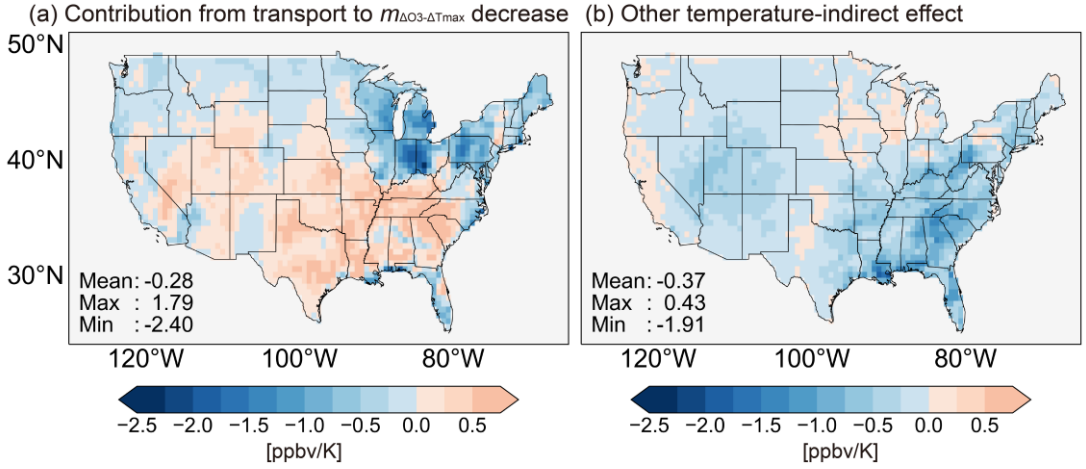

Figure 7. The different temperature-indirect effects for the decrease in $m_{\Delta O3\text{-}\Delta Tmax}$ with anthropogenic NO_x emission reduction. (a) the contribution of the transport to $m_{\Delta O3\text{-}\Delta Tmax}$ decrease with changes in anthropogenic NO_x emissions, estimated as the difference of $m_{\Delta O3\text{-}\Delta Tmax}$ between BASE-TRANS and 1995E-TRANS (Section 2.4). (b) the contribution of the other temperature-indirect effect, estimated as the difference of $m_{\Delta O3\text{-}\Delta Tmax}$ between BASE-FTEMP and 1995E-FTEMP minus the difference between BASE- TRANS and 1995E- TRANS. Mean, maximum, and minimum values of the contributions among all CONUS sites are shown inset.

The temperature-indirect effect on ozone mainly includes the influence of temperature-relevant meteorological parameters such as humidity (as an indicator of content of water vapor) and shortwave radiation on ozone photochemistry, and also the effect of transport (including stagnancy and regional transport). We further distinguish the impact of transport (by normalizing all meteorological elements except three-dimensional wind field and PBLH as input in the GEOS-Chem model) and the other indirect effects on the decrease in $m_{\Delta O3\text{-}\Delta Tmax}$ with emission reduction. As shown in Figure 7, transport (-0.28 ppbv/K) and other indirect effects (-0.37 ppbv/K) such as humidity and radiation show comparable contribution to the decline in $m_{\Delta O3\text{-}\Delta tmax}$, but the spatial patterns show large disparity. The temperature-indirect effect excluding transport (Figure 7b) on $m_{\Delta O3\text{-}\Delta tmax}$ shows a more uniform decline with reduced emissions in most regions across the CONUS, with a larger decrease in Southeast US. This may reflect the impact of solar radiation on BVOCs emission in Southeast US, and its potential for ozone formation reduces with the decline in anthropogenic NO_x emissions. In comparison, the transport effect has larger impacts on the $m_{\Delta O3\text{-}\Delta tmax}$ trend (Figure 7a) with reduced NO_x emissions in the northeastern US, where transport has the largest contribution to the mean $m_{\Delta O3\text{-}\Delta tmax}$ values (Figure S9) as also reported in Kerr et al. (2019), but we find that it causes an increase in $m_{\Delta O3\text{-}}$

https://doi.org/10.5194/egusphere-2024-1889
Preprint. Discussion started: 31 July 2024

$_{\Delta tmax}$ in the southern US. Nevertheless, the impact of transportation on $m_{\Delta O3\text{-}\Delta tmax}$ largely depends on the transportation pattern itself, and it would be more ideally investigated through long-term simulations rather than the one-month study we conducted.

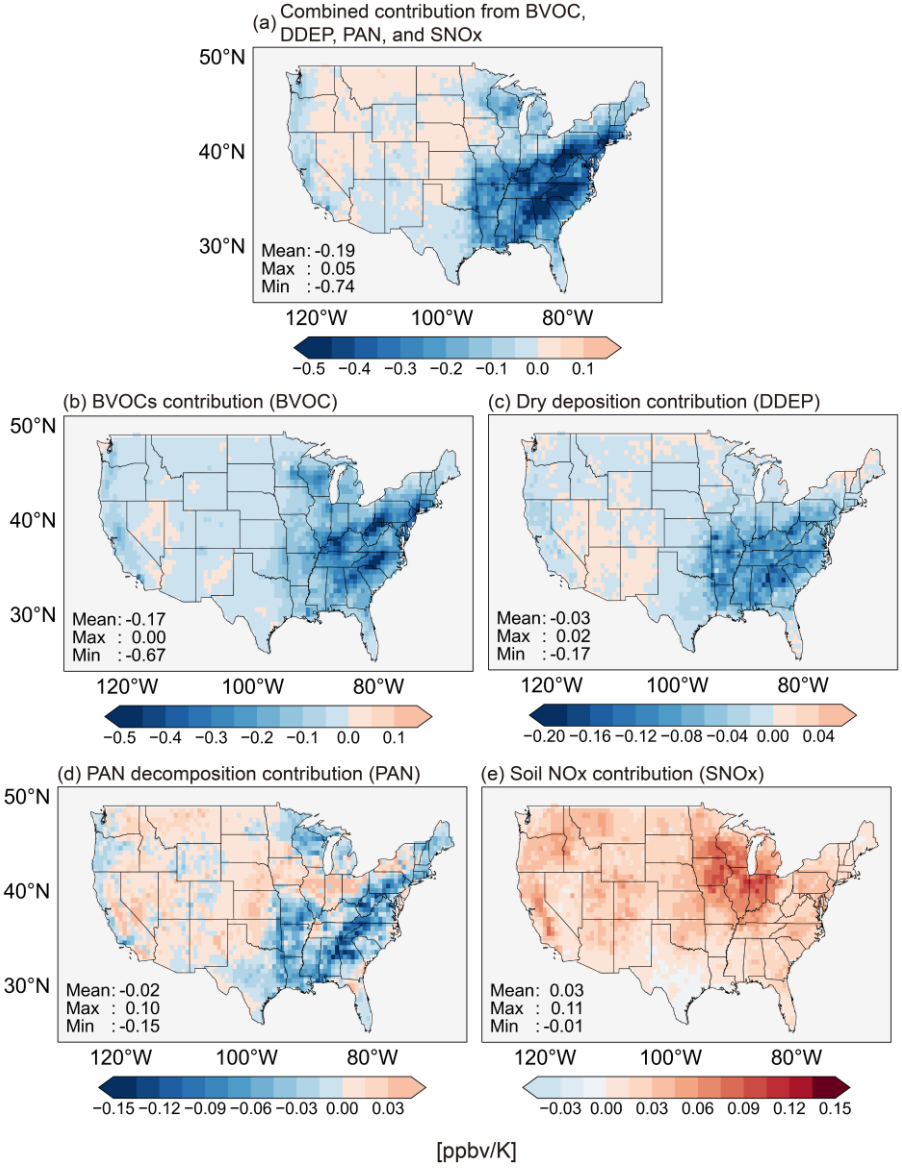

Figure 8. The different temperature-indirect effects for the decrease in $m_{\Delta O3\text{-}\Delta Tmax}$ with anthropogenic NO_x emission reduction. (a) Combined contribution of the four temperature-dependent mechanisms (BVOCs emissions, dry deposition, PAN decomposition, and soil NO_x emissions) to $m_{\Delta O3\text{-}\Delta Tmax}$ with changes in anthropogenic NO_x emissions, estimated as the difference of $m_{\Delta O3\text{-}\Delta Tmax}$ between BASE and 1995E minus the difference between BASE-FALL and 1995E-FALL (Section 2.4). (b)-(e) Individual contribution of BVOCs emissions, dry deposition, PAN decomposition, and soil NO_x emissions) to $m_{\Delta O3\text{-}\Delta Tmax}$ with changes in anthropogenic NO_x

https://doi.org/10.5194/egusphere-2024-1889
Preprint. Discussion started: 31 July 2024

emissions, respectively. Mean, maximum, and minimum values of the contributions among all CONUS sites are shown inset. Note that the data range of each figure is different.

The temperature-direct effects on ozone-temperature sensitivity include the explicit impacts of temperature on BVOCs and soil NOx emissions, chemical kinetics, and dry deposition. Figure 8 shows the additive and individual impacts from the four temperature-dependent mechanisms (BVOCs, dry deposition, PAN decomposition, and soil NOx) on the decrease in $m_{\Delta O3-\Delta tmax}$ decreases with reduced NO_x emissions. Comparison of Figure 8a with Figure 6c shows that the contribution of the four temperature-dependent mechanisms contributes to almost all of the $m_{\Delta O3-\Delta tmax}$ decreases attributable to temperature-direct effect (-0.19 ppbv/K versus -0.21 ppbv/K).

We find that the ozone-temperature sensitivity contributed by BVOCs emissions has significantly reduced with anthropogenic emission control (Figure 8b). In July 2017, BVOCs emissions alone would have contributed to ozone-temperature sensitivity by 0.2 ppbv/K if anthropogenic emissions had remained at 1995 levels, with a particularly large contribution of 0.5 ppbv/K over the parts of eastern US where anthropogenic NO_x emissions are high and ozone formation is sensitivity to VOCs emissions (Figure S10d). However, with anthropogenic NO_x emission decreased to the 2017 level, the contribution of BVOCs emissions decreases to 0.03 ppbv/K averaged over the CONUS sites and -0.01 ppbv/K averaged over the SEUS region (Figure S10c). This suggests that the reduction in anthropogenic NO_x emission has shifted the ozone formation regime to a less VOCs-sensitive state, in which ozone concentrations are much less sensitive to increased BVOCs at high temperatures. Ozone-temperature sensitivity contributed by dry deposition also reduced by -0.03 ppbv/K averaged over the CONUS sites with anthropogenic emission reduction (Figure 8c).

The thermal decomposition of PAN contributes to 0.43 ppbv/K of the overall $m_{\Delta O3-\Delta Tmax}$ over the CONUS (Figure S10g), with larger contribution of 0.7 ppbv/K over the eastern US states. This is also consistent with Porter and Heald (2019), which shows the PAN decomposition explains a large fraction of the ozone-temperature sensitivity compared to other mechanisms such as BVOCs emissions and dry deposition. The PAN concentrations averaged over the CONUS decrease by 27% with the reduction in anthropogenic NO_x emissions (Figure S11). Nevertheless, $m_{\Delta O3-\Delta Tmax}$ contributed by PAN decomposition only shows minor change with the reduction in anthropogenic NO_x emission of -0.02 ppbv/K averaged over the CONUS (Figure 8d), reflecting the offset between $m_{\Delta O3-\Delta Tmax}$ increase in the central and western US and decrease in the eastern US. A possible reason is that, with the reduction of anthropogenic NO_x emissions, ozone formation in the central and western US becomes more NO_x-sensitive, as such the decomposition of PAN increases ozone-temperature sensitivity. The decrease in $m_{\Delta O3-\Delta Tmax}$ contributed by PAN decomposition in the eastern US may mainly reflect the reduction of PAN concentration with anthropogenic NO_x emission reduction (Figure S11).

Unlike the other mechanisms, $m_{\Delta O3-\Delta Tmax}$ contributed by the temperature-dependent soil NO_x emissions increases by 0.03 ppbv/K averaged over the CONUS with anthropogenic NO_x emission reduction. The increase in $m_{\Delta O3-\Delta Tmax}$ reflects the competitive effect between natural soil (from both natural pool and agricultural fertilizer, but are conventionally categorized as natural sources) and anthropogenic (from fossil fuel) NO_x emissions on ozone formation (Lu et al., 2021; Tan et al., 2023).

https://doi.org/10.5194/egusphere-2024-1889
Preprint. Discussion started: 31 July 2024

Soil emissions become an increasingly important source of nitrogen for ozone formation with decreases anthropogenic NO_x emission levels. As soil emissions are larger at higher temperatures, they contribute to an increasing ozone-temperature sensitivity. The above analysis reveals an increasing importance of soil NO_x emissions in determining ozone-temperature sensitivity in a future with low anthropogenic NO_x emissions.

3.4 Ozone mitigation benefit through the declined ozone-temperature sensitivity

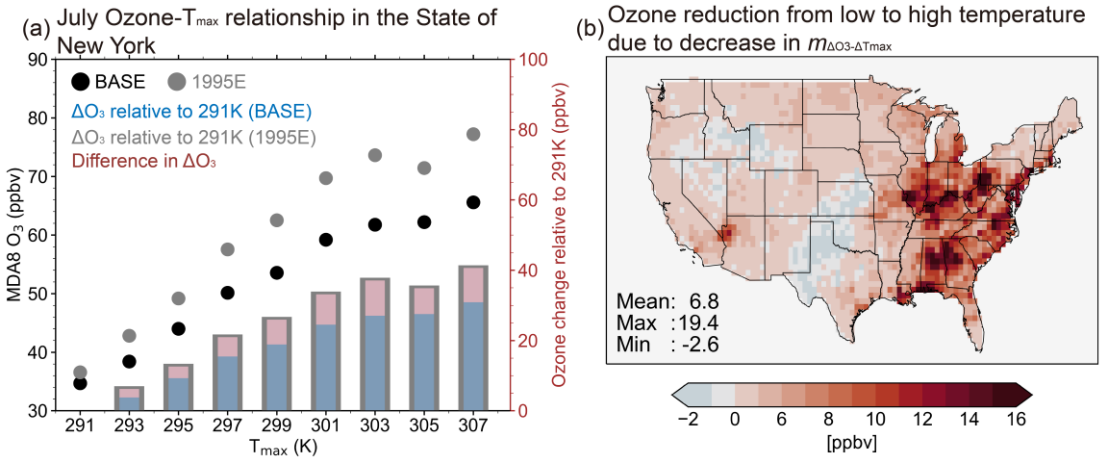

Figure 9. Decreased $m_{\Delta O3\text{-}\Delta Tmax}$ offers ozone mitigation benefit at high temperatures. (a) Simulated ozone concentration in different T_{max} bins in the State of New York in July 2013, 2015, and 2017. Data are binned to 2K intervals. Results from the BASE simulation (black) and 1995E simulation (grey) are shown. The blue bars represent the ozone enhancement for each temperature bin compared to 291K from the BASE simulation. The bar marked by the grey boarder denotes ozone enhancement for each temperature bin compared to 291K from the 1995E simulation. Thus, the red bar (difference between the grey and blue bars) estimated the decrease in ozone enhancement due to the reduction of anthropogenic emissions from 1995 to 2017. (b) Distributions of ozone mitigation benefit in July due to the decreased $m_{\Delta O3\text{-}\Delta Tmax}$, estimated as the ozone enhancement from the lowest 0-10% to 90-100% temperatures bins in the 1995E minus that in the BASE at each grid in July (2013,2015 and 2017). Mean, max, and min values for the 608 sites are shown inset.

The significant decrease in $m_{\Delta O3\text{-}\Delta Tmax}$ over the CONUS indicates that controlling anthropogenic emission not only reduces the mean ozone levels, but also reduces the response of ozone to temperature. Consequently, this reduction lowers the risk of extreme ozone pollution and associated health damage at high temperatures, presenting an appealing benefit for ozone mitigation. We illustrate the benefit by reducing $m_{\Delta O3\text{-}\Delta Tmax}$ in ozone migration taking the State of New York as an example. Figure 9a shows the GEOS-Chem simulated ozone in July for three years (2013, 2015, 2017) at different T_{max} bins. As expected, MDA8 ozone increases with temperature rise. Ozone difference between the highest temperature bin (307K) and the lowest temperature bin (291K) is 31 ppbv in the BASE simulation, comparable to observations (26 ppbv between 307 and 291K). If anthropogenic NO_x emissions were fixed at the 1995 level, however, the predicted ozone difference between the 307K and 291K would be enlarged to 41 ppbv. This means that NO_x emission reductions cause an "additional" ozone concentration reduction of 10 ppbv from 291 to 307 K, as reflected in the significant decline in $m_{\Delta O3\text{-}\Delta Tmax}$. Such benefit of reducing $m_{\Delta O3\text{-}}$

https://doi.org/10.5194/egusphere-2024-1889
Preprint. Discussion started: 31 July 2024

$_{\Delta Tmax}$ is typically larger at higher temperature. Similar phenomenon can be found in other regions with significant decrease in $m_{\Delta O3\text{-}\Delta Tmax}$ (Figure S12).

Figure 9b further quantifies the beneficial effect of anthropogenic emission reduction on ozone mitigation through reducing $m_{\Delta O3\text{-}\Delta Tmax}$ over the CONUS. This can be estimated as the suppression of ozone increase between high (90-100th percentile of T_{max} in July 2013, 2015, 2017) and low temperature range (the lowest 10th percentile of T_{max}) due to anthropogenic NO_x emission reduction from 1995 to 2017. We find that the additional ozone mitigation benefit by reducing $m_{\Delta O3\text{-}\Delta Tmax}$ is 6.8 ppbv averaged across the CONUS. The benefit is more pronounced in the eastern US, where emission reductions are more prominent, reaching a maximum of 19.4 ppbv. The results show that emission controlled on ozone precursors in the US have effectively reduced the ozone surge at high temperatures, and alleviated the combined health damage in the joint occurrences of heat and ozone extremes, highlighting the importance of continuous anthropogenic emission control on ozone mitigation in a warming future.

4. Summary and Discussion

We have estimated in this study the present-day (2017-2021) distributions and long-term (1995-2021) trends in summertime surface ozone-temperature sensitivity in the CONUS, combining observational monitoring network and GEOS-Chem simulations at a resolution of about 50km. We find a clear pattern that the observed $m_{\Delta O3\text{-}\Delta Tmax}$ for the CONUS decreased by 50% from 3.0 ppbv/K in 1990 to 1.5 ppbv/K in 2021 with a mean decreasing rate of -0.57 ppbv/K/decade ($p<0.01$), with urban sites showing faster trends than rural sites (-0.61 vs -0.53 ppbv/K/decade), indicating a much weaker response of ozone to temperature in present-day compared to that in three decades ago. The GEOS-Chem simulations driven by year-specific anthropogenic emission inventory and MERRA-2 reanalysis meteorological fields well reproduce the distribution and magnitude of multi-year mean $m_{\Delta O3\text{-}\Delta Tmax}$, and capture 42% of the observed trends in $m_{\Delta O3\text{-}\Delta Tmax}$ in 1995-2017. The model simulation shows that the decline in anthropogenic NO_x emission over the CONUS is the dominant driver of the $m_{\Delta O3\text{-}\Delta Tmax}$ decrease. Mechanically, approximately 76% of the simulated decline in $m_{\Delta O3\text{-}\Delta Tmax}$ can be attributed to the temperature-indirect effects arising from the shared collinearity of other meteorological effects (such as humidity, ventilation, and transport) on ozone. The remaining portion explaining the decrease in $m_{\Delta O3\text{-}\Delta Tmax}$ with anthropogenic NO_x emission reduction is mostly attributed to four direct temperature-dependent processes, in which $m_{\Delta O3\text{-}\Delta Tmax}$ decrease through the pathways of BVOCs emissions, dry deposition, and PAN decomposition (mostly in the eastern US), while soil NO_x emissions increase $m_{\Delta O3\text{-}\Delta Tmax}$ with anthropogenic NO_x emission reduction.

Our study illustrates that anthropogenic controls on NO_x emissions have significantly reduced the response of surface ozone concentration to the variation of temperature, offering a compelling advantage for ozone mitigation at high temperatures. The model simulation estimates that the reduction of anthropogenic NO_x emissions from 1995 to 2017 decreases the ozone enhancement from low to high temperatures by 6.8 ppbv on average across the CONUS (reaching 19 ppbv in the part of eastern US). The ozone-temperature sensitivity remains a crucial factor in quantifying the impact of climate on ozone. Our research

https://doi.org/10.5194/egusphere-2024-1889
Preprint. Discussion started: 31 July 2024

demonstrates that anthropogenic emission changes not only alleviate current ozone pollution but also help mitigate potential future increases in ozone concentrations due to climate change. It also indicates the dependency of ozone-temperature sensitivity on anthropogenic emission levels that should be considered in projecting future ozone concentration in a warmer climate. Nevertheless, further efforts are needed to enhance the model's ability to capture long-term trends in the ozone response to temperature (including underlying weather conditions and transport patterns), and to better unravel the mechanisms driving the observed ozone-temperature relationship, in particular the role of transport and ventilation.

Data availability

The observational data used in this study is open-access as described in the study. Data from GEOS-Chem modeling that support the findings of this study can be accessed by contacting the corresponding authors (Xiao Lu, luxiao25@mail.sysu.edu.cn).

Acknowledgement

This study is supported by the National Key Research and Development Program of China (2023YFC3706104), Guangdong Basic and Applied Basic Research project (No. 2020B0301030004), and the National Natural Science Foundation of China (42105103)

Author contribution

X.L. designed the study. S.L. performed the model simulations and data analyses with significant input from H.L.W.. S.L. and X.L. wrote the manuscript.

Competing interests.

The contact author has declared that none of the authors has any competing interests

References

Amos, H. M., Jacob, D. J., Holmes, C. D., Fisher, J. A., Wang, Q., Yantosca, R. M., Corbitt, E. S., Galarneau, E., Rutter, A. P., Gustin, M. S., Steffen, A., Schauer, J. J., Graydon, J. A., Louis, V. L. S., Talbot, R. W., Edgerton, E. S., Zhang, Y., and

https://doi.org/10.5194/egusphere-2024-1889
Preprint. Discussion started: 31 July 2024

Sunderland, E. M.: Gas-particle partitioning of atmospheric Hg(II) and its effect on global mercury deposition, Atmospheric Chem. Phys., 12, 591–603, https://doi.org/10.5194/acp-12-591-2012, 2012.

Bey, I., Jacob, D. J., Yantosca, R. M., Logan, J. A., Field, B. D., Fiore, A. M., Li, Q., Liu, H. Y., Mickley, L. J., and Schultz, M. G.: Global modeling of tropospheric chemistry with assimilated meteorology: Model description and evaluation, J. Geophys. Res. Atmospheres, 106, 23073–23095, https://doi.org/10.1029/2001JD000807, 2001.

Bloomer, B. J., Stehr, J. W., Piety, C. A., Salawitch, R. J., and Dickerson, R. R.: Observed relationships of ozone air pollution with temperature and emissions, Geophys. Res. Lett., 36, L09803, https://doi.org/10.1029/2009GL037308, 2009.

Feng, Z., Xu, Y., Kobayashi, K., Dai, L., Zhang, T., Agathokleous, E., Calatayud, V., Paoletti, E., Mukherjee, A., Agrawal, M., Park, R. J., Oak, Y. J., and Yue, X.: Ozone pollution threatens the production of major staple crops in East Asia, Nat. Food, 3, 47–56, https://doi.org/10.1038/s43016-021-00422-6, 2022.

Fiore, A. M., Naik, V., Spracklen, D. V., Steiner, A., Unger, N., Prather, M., Bergmann, D., Cameron-Smith, P. J., Cionni, I., Collins, W. J., Dalsøren, S., Eyring, V., Folberth, G. A., Ginoux, P., Horowitz, L. W., Josse, B., Lamarque, J.-F., MacKenzie, I. A., Nagashima, T., O'Connor, F. M., Righi, M., Rumbold, S. T., Shindell, D. T., Skeie, R. B., Sudo, K., Szopa, S., Takemura, T., and Zeng, G.: Global air quality and climate, Chem. Soc. Rev., 41, 6663–6683, https://doi.org/10.1039/C2CS35095E, 2012.

Fu, T.-M. and Tian, H.: Climate Change Penalty to Ozone Air Quality: Review of Current Understandings and Knowledge Gaps, Curr. Pollut. Rep., 5, 159–171, https://doi.org/10.1007/s40726-019-00115-6, 2019.

Fu, T.-M., Zheng, Y., Paulot, F., Mao, J., and Yantosca, R. M.: Positive but variable sensitivity of August surface ozone to large-scale warming in the southeast United States, Nat. Clim. Change, 5, 454–458, https://doi.org/10.1038/nclimate2567, 2015.

Gaudel, A., Cooper, O. R., Ancellet, G., Barret, B., Boynard, A., Burrows, J. P., Clerbaux, C., Coheur, P.-F., Cuesta, J., Cuevas, E., Doniki, S., Dufour, G., Ebojie, F., Foret, G., Garcia, O., Granados-Muñoz, M. J., Hannigan, J. W., Hase, F., Hassler, B., Huang, G., Hurtmans, D., Jaffe, D., Jones, N., Kalabokas, P., Kerridge, B., Kulawik, S., Latter, B., Leblanc, T., Le Flochmoën, E., Lin, W., Liu, J., Liu, X., Mahieu, E., McClure-Begley, A., Neu, J. L., Osman, M., Palm, M., Petetin, H., Petropavlovskikh, I., Querel, R., Rahpoe, N., Rozanov, A., Schultz, M. G., Schwab, J., Siddans, R., Smale, D., Steinbacher, M., Tanimoto, H., Tarasick, D. W., Thouret, V., Thompson, A. M., Trickl, T., Weatherhead, E., Wespes, C., Worden, H. M., Vigouroux, C., Xu, X., Zeng, G., and Ziemke, J.: Tropospheric Ozone Assessment Report: Present-day distribution and trends of tropospheric ozone relevant to climate and global atmospheric chemistry model evaluation, Elem. Sci. Anthr., 6, 39, https://doi.org/10.1525/elementa.291, 2018.

https://doi.org/10.5194/egusphere-2024-1889
Preprint. Discussion started: 31 July 2024

Gelaro, R., McCarty, W., Suárez, M. J., Todling, R., Molod, A., Takacs, L., Randles, C. A., Darmenov, A., Bosilovich, M. G., Reichle, R., Wargan, K., Coy, L., Cullather, R., Draper, C., Akella, S., Buchard, V., Conaty, A., Silva, A. M. da, Gu, W., Kim, G.-K., Koster, R., Lucchesi, R., Merkova, D., Nielsen, J. E., Partyka, G., Pawson, S., Putman, W., Rienecker, M., Schubert, S. D., Sienkiewicz, M., and Zhao, B.: The Modern-Era Retrospective Analysis for Research and Applications, Version 2 (MERRA-2), J. Clim., 30, 5419–5454, https://doi.org/10.1175/JCLI-D-16-0758.1, 2017.

Gu, Y., Li, K., Xu, J., Liao, H., and Zhou, G.: Observed dependence of surface ozone on increasing temperature in Shanghai, China, Atmos. Environ., 221, 117108, https://doi.org/10.1016/j.atmosenv.2019.117108, 2020.

Guenther, A. B., Jiang, X., Heald, C. L., Sakulyanontvittaya, T., Duhl, T., Emmons, L. K., and Wang, X.: The Model of Emissions of Gases and Aerosols from Nature version 2.1 (MEGAN2.1): an extended and updated framework for modeling biogenic emissions, Geosci. Model Dev., 5, 1471–1492, https://doi.org/10.5194/gmd-5-1471-2012, 2012.

Hudman, R. C., Moore, N. E., Mebust, A. K., Martin, R. V., Russell, A. R., Valin, L. C., and Cohen, R. C.: Steps towards a mechanistic model of global soil nitric oxide emissions: implementation and space based-constraints, Atmospheric Chem. Phys., 12, 7779–7795, https://doi.org/10.5194/acp-12-7779-2012, 2012.

IUPAC: Task group on atmospheric chemical kinetic data evaluation by International Union of Pure and Applied Chemistry (IUPAC), available at: http://iupac.pole-ether.fr/ (last access: 22 June 2023), 2013.

Jacob, D. J. and Winner, D. A.: Effect of climate change on air quality, Atmos. Environ., 43, 51–63, https://doi.org/10.1016/j.atmosenv.2008.09.051, 2009.

Jaffe, D. A., Cooper, O. R., Fiore, A. M., Henderson, B. H., Tonnesen, G. S., Russell, A. G., Henze, D. K., Langford, A. O., Lin, M., and Moore, T.: Scientific assessment of background ozone over the U.S.: Implications for air quality management, Elem. Sci. Anthr., 6, 56, https://doi.org/10.1525/elementa.309, 2018.

Jing, P., Lu, Z., and Steiner, A. L.: The ozone-climate penalty in the Midwestern U.S., Atmos. Environ., 170, 130–142, https://doi.org/10.1016/j.atmosenv.2017.09.038, 2017.

Kerr, G. H., Waugh, D. W., Strode, S. A., Steenrod, S. D., Oman, L. D., and Strahan, S. E.: Disentangling the Drivers of the Summertime Ozone-Temperature Relationship Over the United States, J. Geophys. Res. Atmospheres, 124, 10503–10524, https://doi.org/10.1029/2019JD030572, 2019.

Kim, S.-W., Heckel, A., McKeen, S. A., Frost, G. J., Hsie, E.-Y., Trainer, M. K., Richter, A., Burrows, J. P., Peckham, S. E., and Grell, G. A.: Satellite-observed U.S. power plant NO_x emission reductions and their impact on air quality, Geophys.

https://doi.org/10.5194/egusphere-2024-1889
Preprint. Discussion started: 31 July 2024

Res. Lett., 33, L22812, https://doi.org/10.1029/2006GL027749, 2006.

Leibensperger, E. M., Mickley, L. J., and Jacob, D. J.: Sensitivity of US air quality to mid-latitude cyclone frequency and implications of 1980–2006 climate change, Atmospheric Chem. Phys., 8, 7075–7086, https://doi.org/10.5194/acp-8-7075-2008, 2008.

Lin, M., Horowitz, L. W., Payton, R., Fiore, A. M., and Tonnesen, G.: US surface ozone trends and extremes from 1980 to 2014: quantifying the roles of rising Asian emissions, domestic controls, wildfires, and climate, Atmospheric Chem. Phys., 17, 2943–2970, https://doi.org/10.5194/acp-17-2943-2017, 2017.

Lin, M., Horowitz, L. W., Xie, Y., Paulot, F., Malyshev, S., Shevliakova, E., Finco, A., Gerosa, G., Kubistin, D., and Pilegaard, K.: Vegetation feedbacks during drought exacerbate ozone air pollution extremes in Europe, Nat. Clim. Change, 10, 444–451, https://doi.org/10.1038/s41558-020-0743-y, 2020.

Liu, H., Jacob, D. J., Bey, I., and Yantosca, R. M.: Constraints from 210Pb and 7Be on wet deposition and transport in a global three-dimensional chemical tracer model driven by assimilated meteorological fields, J. Geophys. Res. Atmospheres, 106, 12109–12128, https://doi.org/10.1029/2000JD900839, 2001.

Liu, S., Shu, L., Zhu, L., Song, Y., Sun, W., Chen, Y., Wang, D., Pu, D., Li, X., Sun, S., Li, J., Zuo, X., Fu, W., Yang, X., and Fu, T.-M.: Underappreciated Emission Spikes From Power Plants During Heatwaves Observed From Space: Case Studies in India and China, Earths Future, 12, e2023EF003937, https://doi.org/10.1029/2023EF003937, 2024.

Lu, X., Zhang, L., Chen, Y., Zhou, M., Zheng, B., Li, K., Liu, Y., Lin, J., Fu, T.-M., and Zhang, Q.: Exploring 2016–2017 surface ozone pollution over China: source contributions and meteorological influences, Atmospheric Chem. Phys., 19, 8339–8361, https://doi.org/10.5194/acp-19-8339-2019, 2019a.

Lu, X., Zhang, L., and Shen, L.: Meteorology and Climate Influences on Tropospheric Ozone: a Review of Natural Sources, Chemistry, and Transport Patterns, Curr. Pollut. Rep., 5, 238–260, https://doi.org/10.1007/s40726-019-00118-3, 2019b.

Lu, X., Ye, X., Zhou, M., Zhao, Y., Weng, H., Kong, H., Li, K., Gao, M., Zheng, B., Lin, J., Zhou, F., Zhang, Q., Wu, D., Zhang, L., and Zhang, Y.: The underappreciated role of agricultural soil nitrogen oxide emissions in ozone pollution regulation in North China, Nat. Commun., 12, 5021, https://doi.org/10.1038/s41467-021-25147-9, 2021.

van Marle, M. J. E., Kloster, S., Magi, B. I., Marlon, J. R., Daniau, A.-L., Field, R. D., Arneth, A., Forrest, M., Hantson, S., Kehrwald, N. M., Knorr, W., Lasslop, G., Li, F., Mangeon, S., Yue, C., Kaiser, J. W., and van der Werf, G. R.: Historic global biomass burning emissions for CMIP6 (BB4CMIP) based on merging satellite observations with proxies and fire

https://doi.org/10.5194/egusphere-2024-1889
Preprint. Discussion started: 31 July 2024

models (1750–2015), Geosci. Model Dev., 10, 3329–3357, https://doi.org/10.5194/gmd-10-3329-2017, 2017.

McDuffie, E. E., Smith, S. J., O'Rourke, P., Tibrewal, K., Venkataraman, C., Marais, E. A., Zheng, B., Crippa, M., Brauer, M., and Martin, R. V.: A global anthropogenic emission inventory of atmospheric pollutants from sector- and fuel-specific sources (1970–2017): an application of the Community Emissions Data System (CEDS), Earth Syst. Sci. Data, 12, 3413–3442, https://doi.org/10.5194/essd-12-3413-2020, 2020.

Mills, G., Pleijel, H., Malley, C. S., Sinha, B., Cooper, O. R., Schultz, M. G., Neufeld, H. S., Simpson, D., Sharps, K., Feng, Z., Gerosa, G., Harmens, H., Kobayashi, K., Saxena, P., Paoletti, E., Sinha, V., and Xu, X.: Tropospheric Ozone Assessment Report: Present-day tropospheric ozone distribution and trends relevant to vegetation, Elem. Sci. Anthr., 6, 47, https://doi.org/10.1525/elementa.302, 2018.

Monks, P. S., Archibald, A. T., Colette, A., Cooper, O., Coyle, M., Derwent, R., Fowler, D., Granier, C., Law, K. S., Mills, G. E., Stevenson, D. S., Tarasova, O., Thouret, V., von Schneidemesser, E., Sommariva, R., Wild, O., and Williams, M. L.: Tropospheric ozone and its precursors from the urban to the global scale from air quality to short-lived climate forcer, Atmospheric Chem. Phys., 15, 8889–8973, https://doi.org/10.5194/acp-15-8889-2015, 2015.

Murray, L. T., Jacob, D. J., Logan, J. A., Hudman, R. C., and Koshak, W. J.: Optimized regional and interannual variability of lightning in a global chemical transport model constrained by LIS/OTD satellite data, J. Geophys. Res. Atmospheres, 117, https://doi.org/10.1029/2012JD017934, 2012.

Ning, G., Wardle, D. A., and Yim, S. H. L.: Suppression of Ozone Formation at High Temperature in China: From Historical Observations to Future Projections, Geophys. Res. Lett., 49, https://doi.org/10.1029/2021GL097090, 2022.

Nolte, C. G., Spero, T. L., Bowden, J. H., Sarofim, M. C., Martinich, J., and Mallard, M. S.: Regional temperature-ozone relationships across the U.S. under multiple climate and emissions scenarios, J. Air Waste Manag. Assoc., 71, 1251–1264, https://doi.org/10.1080/10962247.2021.1970048, 2021.

Oikawa, P. Y., Ge, C., Wang, J., Eberwein, J. R., Liang, L. L., Allsman, L. A., Grantz, D. A., and Jenerette, G. D.: Unusually high soil nitrogen oxide emissions influence air quality in a high-temperature agricultural region, Nat. Commun., 6, 8753, https://doi.org/10.1038/ncomms9753, 2015.

Porter, W. C. and Heald, C. L.: The mechanisms and meteorological drivers of the summertime ozone–temperature relationship, Atmospheric Chem. Phys., 19, 13367–13381, https://doi.org/10.5194/acp-19-13367-2019, 2019.

Pusede, S. E., Gentner, D. R., Wooldridge, P. J., Browne, E. C., Rollins, A. W., Min, K.-E., Russell, A. R., Thomas, J., Zhang,

https://doi.org/10.5194/egusphere-2024-1889
Preprint. Discussion started: 31 July 2024

L., Brune, W. H., Henry, S. B., DiGangi, J. P., Keutsch, F. N., Harrold, S. A., Thornton, J. A., Beaver, M. R., St. Clair, J. M., Wennberg, P. O., Sanders, J., Ren, X., VandenBoer, T. C., Markovic, M. Z., Guha, A., Weber, R., Goldstein, A. H., and Cohen, R. C.: On the temperature dependence of organic reactivity, nitrogen oxides, ozone production, and the impact of emission controls in San Joaquin Valley, California, Atmospheric Chem. Phys., 14, 3373–3395, https://doi.org/10.5194/acp-14-3373-2014, 2014.

Pusede, S. E., Steiner, A. L., and Cohen, R. C.: Temperature and Recent Trends in the Chemistry of Continental Surface Ozone, Chem. Rev., 115, 3898–3918, https://doi.org/10.1021/cr5006815, 2015.

Rasmussen, D. J., Fiore, A. M., Naik, V., Horowitz, L. W., McGinnis, S. J., and Schultz, M. G.: Surface ozone-temperature relationships in the eastern US: A monthly climatology for evaluating chemistry-climate models, Atmos. Environ., 47, 142–153, https://doi.org/10.1016/j.atmosenv.2011.11.021, 2012.

Rasmussen, D. J., Hu, J., Mahmud, A., and Kleeman, M. J.: The Ozone–Climate Penalty: Past, Present, and Future, Environ. Sci. Technol., 47, 14258–14266, https://doi.org/10.1021/es403446m, 2013.

Romer, P. S., Duffey, K. C., Wooldridge, P. J., Edgerton, E., Baumann, K., Feiner, P. A., Miller, D. O., Brune, W. H., Koss, A. R., de Gouw, J. A., Misztal, P. K., Goldstein, A. H., and Cohen, R. C.: Effects of temperature-dependent NO_x emissions on continental ozone production, Atmospheric Chem. Phys., 18, 2601–2614, https://doi.org/10.5194/acp-18-2601-2018, 2018.

Sander, S. P., Golden, D., Kurylo, M., Moortgat, G., Wine, P., Ravishankara, A., Kolb, C., Molina, M., Finlayson-Pitts, B., and Huie, R.: Chemical kinetics and photochemical data for use in atmospheric studies, JPL Publ., 06-2, 684 pp., 2011.

Shen, L., Mickley, L. J., and Gilleland, E.: Impact of increasing heat waves on U.S. ozone episodes in the 2050s: Results from a multimodel analysis using extreme value theory, Geophys. Res. Lett., 43, 4017–4025, https://doi.org/10.1002/2016GL068432, 2016.

Sillman, S. and Samson, P. J.: Impact of temperature on oxidant photochemistry in urban, polluted rural and remote environments, J. Geophys. Res., 100, 11497, https://doi.org/10.1029/94JD02146, 1995.

Simon, H., Reff, A., Wells, B., Xing, J., and Frank, N.: Ozone Trends Across the United States over a Period of Decreasing NOx and VOC Emissions, Environ. Sci. Technol., 49, 186–195, https://doi.org/10.1021/es504514z, 2015.

Steiner, A. L., Davis, A. J., Sillman, S., Owen, R. C., Michalak, A. M., and Fiore, A. M.: Observed suppression of ozone formation at extremely high temperatures due to chemical and biophysical feedbacks, Proc. Natl. Acad. Sci., 107, 19685–

https://doi.org/10.5194/egusphere-2024-1889
Preprint. Discussion started: 31 July 2024

19690, https://doi.org/10.1073/pnas.1008336107, 2010.

Tan, W., Wang, H., Su, J., Sun, R., He, C., Lu, X., Lin, J., Xue, C., Wang, H., Liu, Y., Liu, L., Zhang, L., Wu, D., Mu, Y., and Fan, S.: Soil Emissions of Reactive Nitrogen Accelerate Summertime Surface Ozone Increases in the North China Plain, Environ. Sci. Technol., 57, 12782–12793, https://doi.org/10.1021/acs.est.3c01823, 2023.

Travis, K. R. and Jacob, D. J.: Systematic bias in evaluating chemical transport models with maximum daily 8 h average (MDA8) surface ozone for air quality applications: a case study with GEOS-Chem v9.02, Geosci. Model Dev., 12, 3641–3648, https://doi.org/10.5194/gmd-12-3641-2019, 2019.

Turner, M. C., Jerrett, M., Pope, C. A., Krewski, D., Gapstur, S. M., Diver, W. R., Beckerman, B. S., Marshall, J. D., Su, J., Crouse, D. L., and Burnett, R. T.: Long-Term Ozone Exposure and Mortality in a Large Prospective Study, Am. J. Respir. Crit. Care Med., 193, 1134–1142, https://doi.org/10.1164/rccm.201508-1633OC, 2016.

Varotsos, K. V., Giannakopoulos, C., and Tombrou, M.: Ozone-temperature relationship during the 2003 and 2014 heatwaves in Europe, Reg. Environ. Change, 19, 1653–1665, https://doi.org/10.1007/s10113-019-01498-4, 2019.

Wang, Y., Ge, C., Garcia, L. C., Jenerette, G. D., Oikawa, P. Y., and Wang, J.: Improved modelling of soil NOx emissions in a high temperature agricultural region: role of background emissions on NO2 trend over the US, Environ. Res. Lett., 16, 084061, https://doi.org/10.1088/1748-9326/ac16a3, 2021.

van der Werf, G. R., Randerson, J. T., Giglio, L., van Leeuwen, T. T., Chen, Y., Rogers, B. M., Mu, M., van Marle, M. J. E., Morton, D. C., Collatz, G. J., Yokelson, R. J., and Kasibhatla, P. S.: Global fire emissions estimates during 1997–2016, Earth Syst. Sci. Data, 9, 697–720, https://doi.org/10.5194/essd-9-697-2017, 2017.

Wesely, M. L.: Parameterization of surface resistances to gaseous dry deposition in regional-scale numerical models, Atmospheric Environ. 1967, 23, 1293–1304, https://doi.org/10.1016/0004-6981(89)90153-4, 1989.

Wu, S., Mickley, L. J., Leibensperger, E. M., Jacob, D. J., Rind, D., and Streets, D. G.: Effects of 2000–2050 global change on ozone air quality in the United States, J. Geophys. Res., 113, D06302, https://doi.org/10.1029/2007JD008917, 2008.

Wu, W., Fu, T.-M., Arnold, S. R., Spracklen, D. V., Zhang, A., Tao, W., Wang, X., Hou, Y., Mo, J., Chen, J., Li, Y., Feng, X., Lin, H., Huang, Z., Zheng, J., Shen, H., Zhu, L., Wang, C., Ye, J., and Yang, X.: Temperature-Dependent Evaporative Anthropogenic VOC Emissions Significantly Exacerbate Regional Ozone Pollution, Environ. Sci. Technol., https://doi.org/10.1021/acs.est.3c09122, 2024.

Zhang, J., Gao, Y., Leung, L. R., Luo, K., Wang, M., Zhang, Y., Bell, M. L., and Fan, J.: Disentangling the mechanism of

https://doi.org/10.5194/egusphere-2024-1889
Preprint. Discussion started: 31 July 2024

temperature and water vapor modulation on ozone under a warming climate, Environ. Res. Lett., https://doi.org/10.1088/1748-9326/aca3bc, 2022a.

Zhang, J., Gao, Y., Leung, L. R., Luo, K., Wang, M., Zhang, Y., Bell, M. L., and Fan, J.: Isolating the modulation of mean warming and higher-order temperature changes on ozone in a changing climate over the contiguous United States, Environ. Res. Lett., 17, 094005, https://doi.org/10.1088/1748-9326/ac8695, 2022b.

Zhang, L., Jacob, D. J., Yue, X., Downey, N. V., Wood, D. A., and Blewitt, D.: Sources contributing to background surface ozone in the US Intermountain West, Atmospheric Chem. Phys., 14, 5295–5309, https://doi.org/10.5194/acp-14-5295-2014, 2014.

Zhang, X., Waugh, D. W., Kerr, G. H., and Miller, S. M.: Surface Ozone-Temperature Relationship: The Meridional Gradient Ratio Approximation, Geophys. Res. Lett., 49, e2022GL098680, https://doi.org/10.1029/2022GL098680, 2022c.